Atmos. Chem. Phys., 9, 4467–4483, 2009
www.atmos-chem-phys.net/9/4467/2009/

Atmospheric Chemistry and Physics

Exploring atmospheric boundary layer characteristics in a severe SO_2 episode in the north-eastern Adriatic

M. T. Prtenjak[1], **A. Jeričević**[2], **L. Kraljević**[2], **I. H. Bulić**[1], **T. Nitis**[3], **and Z. B. Klaić**[1]

[1]Andrija Mohorovičić Geophysical Institute, Department of Geophysics, Faculty of Science, University of Zagreb, Croatia
[2]Meteorological and Hydrological Service of Croatia, Zagreb, Croatia
[3]Laboratory of Geoinformatics and Environmental Application, Department of Marine Sciences, University of the Aegean, 81100 Mytilene, Greece

Received: 23 December 2008 – Published in Atmos. Chem. Phys. Discuss.: 9 March 2009
Revised: 1 July 2009 – Accepted: 6 July 2009 – Published: 13 July 2009

Abstract. Stable atmospheric conditions are often connected with the occurrence of high pollution episodes especially in urban or industrial areas. In this work we investigate a severe SO_2 episode observed on 3–5 February 2002 in a coastal industrial town of Rijeka, Croatia, where very high daily mean concentrations (up to 353.5 $\mu g\,m^{-3}$) were measured. The episode occurred under high air pressure conditions, which were accompanied with a fog and low wind speeds. Three air quality models (50-km EMEP model, 10-km EMEP4HR model and 1-km CAMx model) were used to simulate SO_2 concentrations fields and to evaluate the relative contribution of distant and local pollution sources to observed concentrations. Results suggest that the episode was caused predominately by local sources. Furthermore, using three-dimensional, higher-order turbulence closure mesoscale meteorological model (WRF), the wind regimes and thermo-dynamical structure of the lower troposphere above the greater Rijeka area (GRA) were examined in detail. Modelled atmospheric fields suggest several factors whose simultaneous acting was responsible for elevated SO_2 concentrations. Established small scale wind directions supported the transport of air from nearby industrial areas with major pollution sources towards Rijeka. This transport was associated with strong, ground-based temperature inversion and correspondingly, very low mixing layer (at most up to about 140 m). Additionally, the surface winds in Rijeka were light or almost calm thus, preventing ventilation of polluted air. Finally, a vertical circulation cell formed between the mainland and a nearby island, supported the air subsidence and the increase of static stability.

Correspondence to: M. T. Prtenjak
(telisman@irb.hr)

1 Introduction

Facing the Adriatic Sea and surrounded by mountains (Fig. 1), Rijeka is a coastal industrial town situated in a region of very complex wind regimes (e.g. Klaić et al., 2003; Nitis et al., 2005; Prtenjak et al., 2006, 2008; Prtenjak and Grisogono, 2007; Klaić et al., 2009). In the Greater Rijeka Area (GRA), southeast of the Rijeka town, some of the major individual sources of SO_2 in Croatia are found, such as an oil refinery and a thermal power plant. According to estimates from the Ministry of Environmental Protection, Physical Planning and Construction of the Republic of Croatia (http://www.mzopu.hr, data for 2002) the two sources emit about 20% of the total national emissions of SO_2, where 8933 and 4909 tones of SO_2 correspond to the oil refinery and thermo-power plant, respectively. In addition, compared to other regions along the eastern Adriatic coast, the GRA – together with the Istria peninsula – is more exposed to the long-range transport of pollutants from western Europe (e.g. Klaić, 1990, 1996; Klaić and Beširević, 1998; Klaić, 2003).

In terms of air quality protection, knowledge of the basic characteristics of the wind and thermodynamic conditions is essential, especially in cases of severe air pollution episodes (Skouloudis et al., 2009). An air pollution episode is defined as an event in which concentrations of air pollutants increase substantially above the national standard limit (Fisher

Published by Copernicus Publications on behalf of the European Geosciences Union.

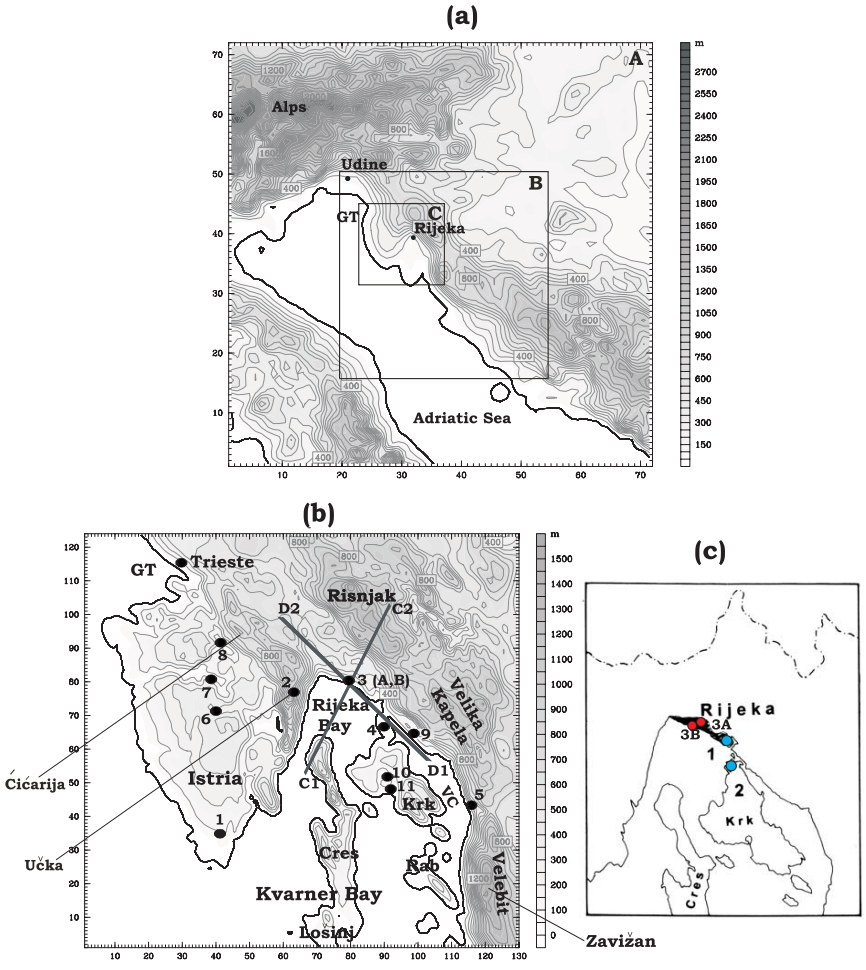

Fig. 1. (a) Configuration of nested WRF domains at the north-eastern Adriatic coast. Frames indicate the coarse (A), medium (B) and the fine (C) WRF model domain, respectively. **(b)** Anaglyph for the fine-grid domain. Positions of routine measuring sites are shown by filled black circles (see text for details). Lines C1C2 and D1D2 show bases of vertical cross-sections investigated in the Sect. 5. **(c)** Major industrial areas in the Greater Rijeka Area (GRA) are shown by filled blue circles: 1 – industrial zone of Rijeka with, among others, an oil refinery and thermo-power plant, 2 – Petrochemical plant and the oil terminal (Omišalj, Krk island). The town of Rijeka is hatched in black and the position of the two measuring sites in Rijeka (3A and 3B) is presented by circles filled in red.

et al., 2005). Pollution episodes can occur due to various causes, such as, increased pollutant emissions, topographical (e.g. Brulfert et al., 2005) and/or thermal forcing (e.g. Robinsohn et al., 1992; Evtyugina et al., 2006; Drobinski et al., 2007; Levy et al., 2008), favourable weather conditions and season or chemical characteristics of the atmosphere. Results of many studies (e.g. Robinsohn et al., 1992; Soler et al., 2004; Pohjola et al., 2004; Fisher et al., 2005; Tayanc and Bercin, 2007) showed that severe air pollution episodes around the world are very often associated with high pressure conditions, weak winds and/or strong low-level temperature inversion and poor vertical mixing (e.g. Natale et al., 1999). In some cases occurrence of high level SO_2 episodes have been caused by long range transport (e.g., Steenkist, 1988; De Leeuw and Leyssius, 1989).

A human health risk event occurred in Rijeka during 3 to 5 February 2002, where a daily mean concentration of SO_2 reached the value of $353.5\,\mu g\,m^{-3}$, which is about 10 times the average daily value in February and more than twice of a limit value of $125\,\mu g\,m^{-3}$ prescribed by a law (http://www.zzjzpgz.hr/zrak/index.php). Therefore, on 4 February, the local authorities warned Rijeka inhabitants to remain indoors. Managements of the oil refinery and thermal power plant claimed that during the episode their emissions were at normal levels.

A previous study of the same episode (Jeričević et al., 2004) suggested fumigation due to high pressure conditions and consequent weak circulation as the cause. However, their study was based on simulations provided by the operational hydrostatic numerical weather forecast model ALADIN (*Aire Limitée Adaptation dynamique Développement*

Table 1. Measuring sites in the north-eastern Adriatic (see also Fig. 1). A station type (ST) is given by abbreviations: M, O, AQ and RS for the main meteorological station, ordinary meteorological station, air quality monitoring and radio-sounding station, respectively. Temporal resolution (T) of the ordinary meteorological station corresponds to the three following terms: 06:00 UTC, 13:00 UTC and 20:00 UTC.

Site code	Site name	ST	T (h)	Lat	Long	a.s.l. (m)	Geographical specifications
1	Pula-airport	M	24	44.9°	13.9°	63	SW Istrian coast near tip of peninsula, 10 km from the NW coast
2	Učka	M	24	45.3°	14.2°	1372	at top of the mountain of Učka
3A	Rijeka	M	24	45.3°	14.5°	120	at the eastern side of the Rijeka Bay 1 km far from the coast
3B	Rijeka	AQ	24	45.3°	14.4°	20	at the coast at the eastern side of the Rijeka Bay
4	Rijeka-airport	M	8	45.2°	14.5°	85	2 km from the NW coast at the island of Krk
5	Senj	M	24	44.9°	14.9°	26	on the borderline between two mountains – Velika Kapela and Velebit, 0.5 km from the coast
6	Pazin	O	3	45.2°	13.9°	291	in the very centre of Istrian peninsula, 30 km from the coast
7	Botonega	O	3	45.3°	13.9°	50	in the wind protected area near small river lake in the middle of Istria
8	Abrami	O	3	45.4°	13.9°	85	in the wind protected area in the middle of Istria
9	Crikvenica	O	3	45.2°	14.7°	2	in the coastal zone squeezed between the sea and the island of Krk,
10	Ponikve	O	3	45.1°	14.6°	25	northward above town Krk near the SE coast,
11	Krk	O	3	45.0°	14.6°	9	at the SE coast of the island of Krk
12	Udine	RS	4	46.0°	13.2°	94	in the hinterland in Italy

InterNational) (Geleyn et al., 1992) at horizontal resolution of 8 km, and accordingly smoothed terrain topography. Thus, it did not offer a detailed insight in the fine-scale ($\sim$1 km) lower-tropospheric conditions responsible for this particular pollution event, which, we believe, we have succeeded in doing in the present study.

Another novelty of this study, compared to the investigation of Jeričević et al. (2004), is an assessment of the relative contribution of distant pollution sources in the occurrence of the observed elevated SO_2 concentrations. For this purpose, we applied the Unified European Monitoring and Evaluation Programme (EMEP) model (www.emep.int) that simulates atmospheric transport and deposition of pollutants at regional and synoptic scale. Apart from the EMEP modelled fields at $50\times50\,km^2$, thanks to the ongoing EMEP4HR project (Jeričević et al., 2007), we utilized preliminary EMEP4HR model results at $10\times10\,km^2$ resolution. In addition, we investigated the fine scale ($1\times1\,km^2$) results obtained by widely used (e.g. de Foy et al., 2007) small scale Comprehensive Air quality Model with extensions (CAMx) (http://www.camx.com/).

2 Study area and data

The GRA is located in the western part of Croatia (Fig. 1a) and it is characterized by a complex topography. It is a mountainous area open to the sea towards the south, where several islands are located, with Cres and Krk being the largest (Fig. 1b). The Rijeka urban area faces the Kvarner Bay. The Kvarner Bay is surrounded with rather high mountains with steep slopes: Risnjak (more than 1250 m high), Velika Kapela (1534 m) and Velebit (1758 m). Westward from Rijeka, the terrain rises very abruptly along the coastline (Učka and Ćićarija mountains, 1401 m, and 1272 m, respectively), forming a physical boundary between the Istria peninsula and the Kvarner Bay. A more gradual rise of the terrain is found north-west of the Rijeka urban area, with an elevation of less than 500 m a.s.l., where a roughly triangular valley extends towards the Gulf of Trieste (GT in Fig. 1b), which is near the north-western boundary of the study area.

Meteorological data from main and ordinary meteorological stations in the north-eastern Adriatic region were used in order to investigate the temporal variations of the wind field. The details on measuring sites are listed in Table 1, and their locations are shown in Fig. 1b.

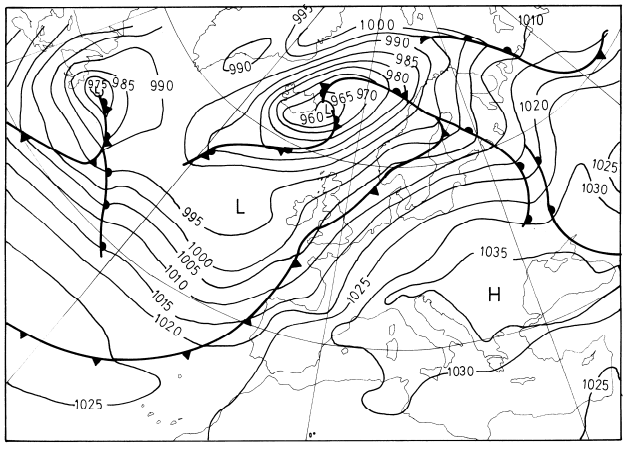

Fig. 2. Surface diagnostic chart for Europe at 00:00 UTC on 3 February 2002 (source: European Meteorological Bulletin).

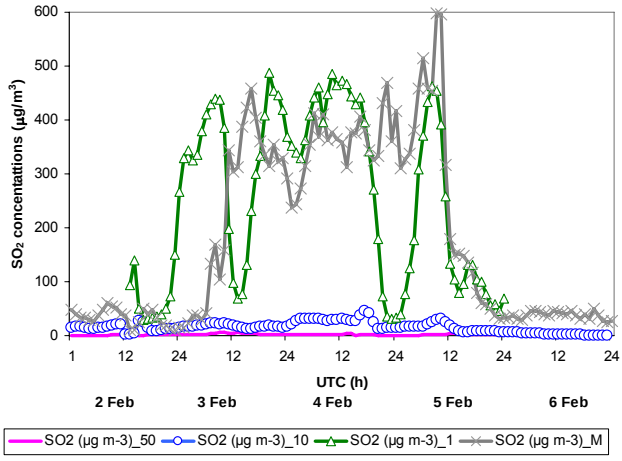

Fig. 3. Hourly SO_2 concentrations for Rijeka from 2 to 6 February 2002: EMEP at 50-km resolution (pink solid line), EMEP4HR at 10-km resolution (blue line with circles), CAMx at 1-km resolution (green line with triangles), and, measured at the site 3B in Table 1 and Fig. 1b (grey line with crosses) (source: Teaching Institute for Public Health, Rijeka).

Meteorological charts over Europe for the period of study show a high pressure field over the central and south-eastern part of Europe. Here we show only one snapshot of the surface conditions over Europe (Fig. 2). Over the north-eastern Adriatic coast these were accompanied by weak pressure gradients and consequently, weak surface winds, and stagnant conditions with fog and low stratified cloudiness. On 5 February, the high pressure field started to weaken, indicating the change of synoptic forcing due to the Genoa Cyclone that approached the Kvarner Bay (not shown). Additionally, the radio-sounding performed in Udine (coarse domain; Fig. 1a) revealed a high static stability ranging from 5.6 K km^{-1} on 2 February to 5.2 K km^{-1} on 5 February. During the entire period under study, the winds in the lowermost 2 km in Udine were mostly less than 4 m s^{-1}, and varied from south-westerly to westerly.

In the studied area, a few episodes with the high levels of SO_2 (daily means between 130–143 μg m^{-3}) usually occur during the wintertime (e.g. 15 December 2006, 6 January 2007, 20 January 2008; http://zrak.mzopu.hr/default.aspx?id=22). Nevertheless, the episode investigated here is characterized by unusually high SO_2 concentrations (Fig. 3), and thus, it could not be considered as typical. As of 3 February 08:00 UTC, the SO_2 concentration started to increase. After continuous growth, on 5 February at 09:00 UTC it reached the hourly maximum of about 600 μg m^{-3}. As of 5 February 11:00 UTC concentrations started to decrease. Thus, after 12:00 UTC they were below 150 μg m^{-3}. This pollutant concentration decrease coincided with the change of the large-scale, synoptic conditions. The highest daily mean concentration occurred on 4 February. It reached a value of 353.5 μg m^{-3}, which is about 10 times higher than the average.

3 Air quality models

3.1 The standard EMEP model

The daily SO_2 concentrations have been calculated by the Unified EMEP model (http://www.emep.int/) which was developed at the Norwegian Meteorological Institute (MET. NO.). The EMEP model is a multi-layer dispersion model which simulates the long-range transport and deposition of air pollution i.e. acidifying and eutrophying compounds, photo-oxidants and particulate matter, providing critical levels of pollutant concentrations at a daily scale for regulatory purposes. The model is fully documented (e.g. Simpson et al., 2003; Fagerli et al., 2004). The EMEP domain covers Europe and the Atlantic Ocean, with a horizontal resolution of 50 km and with 20 terrain-following layers in vertical up to 100 hPa. The meteorological input is obtained every 3 h, from the PARallel Limited Area Model with Polar Stereographic map projection (PARLAM-PS), a dedicated version for EMEP of the HIgh Resolution Limited Area Model (HIRLAM) numerical weather prediction model. The simulated species are calculated by 4th and 2nd order Bott (1989a, b) advection scheme which is based on the O'Brien function (1970) in unstable PBL, while Blackadar diffusion scheme is used for stable condition and outside PBL. The necessary anthropogenic emissions input for SO_2, NO_x, CO, NH_3, Non-methane Volatile Organic Compounds (NMVOC) and particulates are specified according to the annual national emissions reported per sector and grid.

3.2 The EMEP4HR model

Currently, considerable scientific effort is being invested in the further development of the EMEP modelling system in order to make it applicable at finer resolutions (i.e. national scales and finer time scales). At the moment, there are two such ongoing joint projects: one for the UK domain (EMEP4UK, Vieno et al., 2008, 2009), and the other for Croatia (EMEP4HR, Jeričević et al., 2007). Here, we have applied the Unified EMEP model version for the smaller domain, a setup called EMEP4HR. This is continuing effort, and results of the EMEP4HR model setup are still considered preliminary. The model was run at 10-km horizontal resolution for the domain that is relevant for Croatia. A hydrostatic NWP model ALADIN (Geleyn et al., 1992), which is run operationally at the Croatian Meteorological and Hydrological Service at a horizontal resolution of 8 km, was used as a meteorological driver. Meteorological fields are updated every 3 h. The EMEP model was run with the same resolution and projection (tangent version of Lambert conformal projection) as the meteorological driver. Thus, no horizontal interpolation of the meteorological fields was done during the preprocessing of meteorological fields. In vertical, meteorological fields were interpolated to the EMEP model levels which are the same as in the standard Unified EMEP model setup. The EMEP4HR setup is nested in the standard EMEP domain; 1-way nesting was used, with the coupling frequency of 1 h. For the purpose of EMEP4HR project (Jeričević et al., 2007), the new, high resolution (10-km grid) emission inventory for Croatia was performed. Outside of Croatia, the EMEP emissions at 50-km resolution are interpolated to 10-km grid. Thus, local Croatian sources are resolved much better than the local sources in other countries within the investigated domain.

3.3 The CAMx model

To obtain the high-resolution hourly SO_2 concentrations in this very complex zone (topography, land/sea interface, land use), Comprehensive Air Quality Model with extensions (CAMx, version 4.51) was employed (e.g. de Foy et al., 2007; ENVIRON, 2008). It is widely used Eulerian photochemical dispersion model. Simulations were made with the Carbon Bond IV mechanism (Gery et al., 1989), Piecewise Parabolic Method (PPM) horizontal advection solver and Chemical Mechanism Compiler (CMC) chemistry solver. The meteorological input was obtained from nonhydrostatic WRF model (see Sect. 4) for every hour. The CAMx was run on a domain identical to the finest WRF domain (frame C in Fig. 1a) at 1 km horizontal resolution with the first 15 of the 65 vertical levels used in WRF model setup. These correspond to approximately 3700 m deep layer above the surface. Emission fields were taken from 10-km resolution emission inventory for Croatia (i.e. EMEP4HR emissions, Sect. 3.2), and they were linearly interpolated to 1-km resolution.

4 Mesoscale meteorological model

Small-scale meteorological conditions were simulated by the mesoscale Weather Research and Forecasting model (version 2.2) (WRF, http://www.wrf-model.org/index.php; Skamarock et al., 2007). The WRF model is used in a variety of areas (Michalakes et al., 2004) including storm prediction and research (e.g. Kain et al., 2006), air-quality modelling (e.g. Jimenez-Guerrero et al., 2008), wildfire, hurricane (e.g. Trenberth et al., 2007), tropical storm prediction and regional climate and weather prediction (e.g. Skamarock and Klemp, 2008). The WRF model consists of fully compressible nonhydrostatic equations on a staggered Arakawa C grid. Thus, the wind components u, v, and w are recorded at the respective cell interfaces and all other variables, as volumetric cells, carry averages at the cell centre. Its vertical coordinate is a terrain-following hydrostatic pressure coordinate. Here, the model uses the Runge-Kutta 3rd order time integration scheme and 5th order advection schemes in horizontal direction and the 3rd order in vertical ones. A time-split small step for acoustic and gravity-wave modes is utilized. The dynamics conserve scalar variables.

In this study a two-way nested option was used, where a horizontal step of the coarse domain was 9-km (on the Lambert conformal projection). The coarse domain of 648 km×648 km covers the major portion of the Adriatic Sea area (frame A in Fig. 1a). The medium domain of 318 km×318 km with a horizontal resolution of 3 km covers the Kvarner Bay (frame B in Fig. 1a). The fine-grid domain corresponds to an area of 130 km×124 km and 1 km horizontal resolution (frame C in Fig. 1a), and it captures the GRA, including the major SO_2 sources. With the resolution of 1 km, the ratio of the energy-containing turbulence scale and the scale of the spatial filter used on the equations of motion is small. It should mostly prevent the overlapping effect between the TKE parameterization and the resolved boundary layer (e.g. Wyngaard, 2004). The finest resolution of 1 km and the ratio (1:3) determine the horizontal resolution of two larger model grids, which were used solely to produce initial and boundary conditions for the finest grid. Sixty-five terrain-following coordinate levels were used with the lowest level at about 25 m. The spacing between levels gradually increases from 50 m at the bottom to 300 m in the middle and upper troposphere, and finally to 400 m toward the top that was set at 20 km. The WRF dynamical and physical options used for all three domains are: the ARW dynamical core; the Mellor-Yamada-Janjic (MYJ) scheme for the planetary boundary layer (PBL); the rapid radiative transfer model for the long-wave radiation and the Dudhia scheme for short-wave radiation; the single-moment 3-class microphysics' scheme with ice and snow processes; the Eta surface layer scheme based on the Monin-Obukhov theory and the five-layer thermal diffusion scheme for soil temperature. For the coarse 9-km domain the Betts-Miller-Janjic cumulus parameterization is employed, however without parameterization

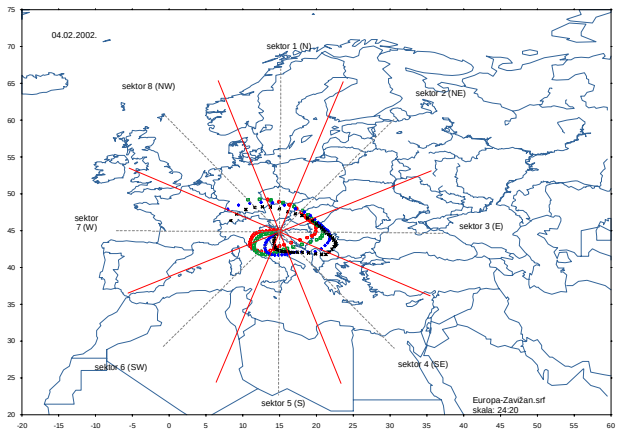

Fig. 4. 4-day backward 925 hPa trajectories arriving at the EMEP site closest to Rijeka (Zavižan, see Fig. 1b) on 4 February 2002, at 00:00 UTC (black), 06:00 UTC (blue), 12:00 UTC (green) and 18:00 UTC (red). Parcel positions are given for every second hour.

in the inner domains. Initialization and boundary conditions were taken from the European Centre for Medium-Range Weather Forecasts (ECMWF) Reanalysis fields. The ECMWF data were available at a 0.25-degree resolution (∼25 km resolution) at the standard pressure levels every 6 h. Simulation was performed from 12:00 UTC of 31 January to the 00:00 UTC of 6 February. During the studied period, the observed sea surface temperatures were almost constant in time and space (∼9.5° C). Therefore, the WRF version with the time-constant sea surface temperature was employed.

5 Results and discussion

5.1 Air quality

According to Fig. 3, the observed daily concentration of SO_2 started to increase considerably on 3 February 2002.The first step was to evaluate a possible contribution of the long-range SO_2 transport which is provided by the 50-km EMEP model. The EMEP modelled concentrations show a very small increase during the episode (e.g. at the beginning of the episode on 3 February, Fig. 3). In addition, air trajectories for selected EMEP sites are operationally calculated by tracking an air parcel every 2 h for 96 h backwards in time for 4 different starting times, i.e. 00:00 UTC, 06:00 UTC, 12:00 UTC and 18:00 UTC. For each single term, two-dimensional trajectories are defined by a total of 49 position points (including the arrival point). Trajectory calculations are based on modelled wind fields at mean sigma level of 0.925 obtained from the model PARLAMPS in the EMEP grid developed at the MET. NO. Trajectories (Fig. 4) show that approximately 2 days before the occurrence of the episode, the air parcels were passing above the known main regional SO_2 emission areas in Hungary, Bulgaria and central Bosnia, as well as central Italy. Consecutive parcel positions are very close, especially for the last 24 h. This suggests the low modelled wind speeds ($<5\,m\,s^{-1}$) and stagnant conditions over the wider region, which is in accordance with the high pressure system (Fig. 2). Different starting times of trajectories revealed westward shift. However, the 50-km EMEP modelled values comprised only up to about of 2% of the observed concentrations, suggesting that the majority of the observed high SO_2 concentrations arise from local emission sources. The same is further corroborated with EMEP4HR results, although the contribution of non-local pollution sources to pollutant concentrations is somewhat larger (up to about 10%). Furthermore, CAMx modelled concentrations, which are due to pollution sources within the domain shown in Fig. 1b (i.e., mainly sources within the GRA) agree reasonably well with measured values.

Table 2 shows statistics for the employed models namely, mean diurnal value, maximum value, root mean square error (RMSE), correlation coefficient and index of agreement, d, (e.g. Willmott, 1982), while Fig. 5 illustrates a snapshot of horizontal distribution of hourly SO_2 fields for the three air quality models. The d-index determines the degree to which the observed value is accurately estimated by the simulated value, and is a measure of the degree to which a model's predictions are error free. Values of d-index are in the range of 0.0, when there is no agreement between the observed and the predicted values, and 1.0 which represents perfect agreement between observed and predicted values. Similar to Fig. 3, both Table 2 and Fig. 5 also show that: 1) the agreement between modelled and measured values, as expected, increase with the model resolution. (Namely, apart from the more realistic representation of emission fields, the increased model resolution also generally implies better incorporation of input data, such as, topography, land-use etc.; and, consequent meteorological files); and 2) the local emission sources played the major role in the establishment of the investigated episode. (For Rijeka, the mean CAMx modelled concentration (i.e. caused by sources within the GRA) over the entire period was 252.5 $\mu g\,m^{-3}$, while corresponding measured value is 242.4 $\mu g\,m^{-3}$. Simultaneously, mean concentrations in Rijeka, caused by the central European sources and entire Europe were, 18.7 and 22.2 $\mu g\,m^{-3}$, respectively.)

5.2 Meteorological conditions

5.2.1 Measured vs. modelled data

In order to validate the WRF simulation results, we compared them to the available surface observations furnished by the main meteorological stations in the fine-grid domain (shown in Fig. 1b). Table 3 presents only one statistic index, the d-index among others calculated statistic indices (not shown). The shown parameter in Table 3 reflects the degree to which measurements are accurately estimated by

Table 2. Statistic indices for modelled and measured SO_2 concentrations.

	Mean values ($\mu g\,m^{-3}$)	Maximum values ($\mu g\,m\text{-}^{3}$)	Correlation coefficient	RMSE	d-index of agreement
EMEP_50-km	2.2	6.2	0.2	292.3	0.5
EMEP4HR_10-km	18.7	45.4	0.5	276.5	0.5
CAMx_1-km	252.5	487.6	0.5	175.1	0.7
Measurements	242.4	597.5	–	–	–

Table 3. Index of agreement for the wind speed, wind direction and 2-m air temperature, respectively, modelled by WRF model during period 2–5 February 2002. This statistic index reflects the degree to which measurements are accurately estimated by the model.

Site code	Site name	Wind speed	Wind dir	Temp
1	Pula-airport	0.7	0.9	0.5
2	Učka	0.5	0.9	–
3A	Rijeka	0.3	0.8	0.6
5	Senj	0.5	0.9	0.8

the model. The calculations were made for wind speed, wind direction and temperature at four stations with 24 h measurements. During 2–5 February, the d-index, for all the aforementioned variables showed reasonable model performance, although somewhat poorer agreement was obtained for the wind speed in the 3A (Rijeka) site (Table 3 and Fig. 6a). At this site, Fig. 6b, wind direction is reproduced reasonably well. Due to low wind speeds, the measured wind directions are highly variable, while the modelled ones are more organized into local flows. Such recorded low wind speeds ($<2\,m\,s^{-1}$) are generally difficult to model (e.g. Mahrt and Vickers, 2006; Mahrt, 2007). The smoothing of the model terrain at the 1-km resolution, and the parameterization of turbulent fluxes during the night in the stable boundary layer according to the Monin-Obukhov theory (e.g. Grisogono et al., 2007; Baklanov and Grisogono, 2007) are the most probable causes. The air temperature at 2 m in Rijeka is generally overestimated (Fig. 6c). Still the agreement is acceptable (Table 3) especially in respect to the local observed fog formation, weak winds and almost equal sea and air surface temperatures during the studied period. Finally, knowing the overwhelmingly complex terrain, finite resolution of the model and its parameterizations, the overall correspondence between measurements and the WRF model is satisfactory.

5.2.2 Horizontal fields

On 2 February sunny conditions were observed in the GRA and the maximum air temperature there was higher than the sea surface temperature by 10°C. Thus, a growth of the mixed layer is expected, which is potentially accompanied by the mixing down of elevated pollutants present in the residual layer from the previous day (Stull, 1988). Jeričević et al. (2004) assumed that the observed SO_2 concentration growth on 3 February was due to pollutant entrainment into the boundary layer from the residual layer of previous day. Still, their model results did not allow final conclusion. Since the maximum concentration occurred on the 4 February, we mostly focus on the lower-tropospheric conditions during the pollution episode, from 2 to 4 February 2002. Figure 7 shows the simulated 10-m wind field on 2 February 2002 at 13:00 UTC. Both measurements and simulation results show prevailing north-westerly winds over the western part of the Istria peninsula (Fig. 7a). The simulated wind field suggests an advection of the marine moist air towards land, which explains the observed fog above the western Istrian coast.

However, the WRF model slightly overestimated the measured air surface temperature over west Istria (not shown here). Compared to the west coast, above the central part of the Istria peninsula, both measured and simulated (Fig. 7b) maximum daily temperatures are higher. Such a temperature pattern extends towards the GRA, where the model values are slightly lower than the measured ones. Regarding the wind field, (Fig. 7a), blocking is established at the windward side of mountains Ćićarija, Učka and Risnjak. Owing to the upstream blocking inside a roughly triangular valley stretching toward the Gulf of Trieste, the winds are weak. Between the island of Cres and Istria the wind veers toward south-westerly. Over the western, lee sides of the Učka mountain, the island of Cres and over a large portion of the Velika Kapela and Velebit mountains, the downslope accelerated flow is found due to radiative cooling of the mountain slopes. Above Rijeka, the north-eastern flow meets the south-westerly winds blowing over the Rijeka Bay resulting in an onshore flow above the coastline. Although light, these winds ventilated the GRA, and thus, daily SO_2 concentration on 2 February was relatively low (Fig. 3). Between the is-

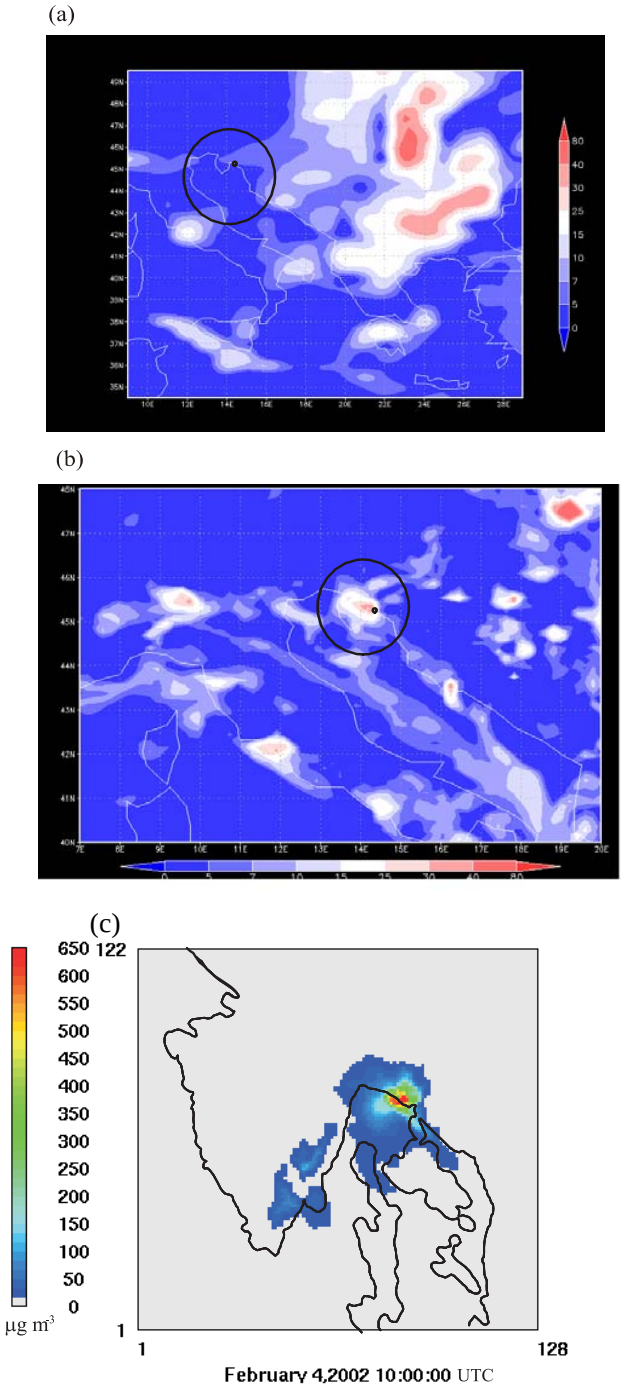

Fig. 5. The horizontal distribution of hourly surface SO_2 concentrations ($\mu g\,m^{-3}$) for 4 February 2002 at 10:00 UTC **(a)** 50-km EMEP model; **(b)** 10-km EMEP4HR model; and, **(c)** 1-km CAMx model. The black circles and black dots at two upper panels display the studied area (north-eastern Adriatic) and the position of Rijeka town, respectively.

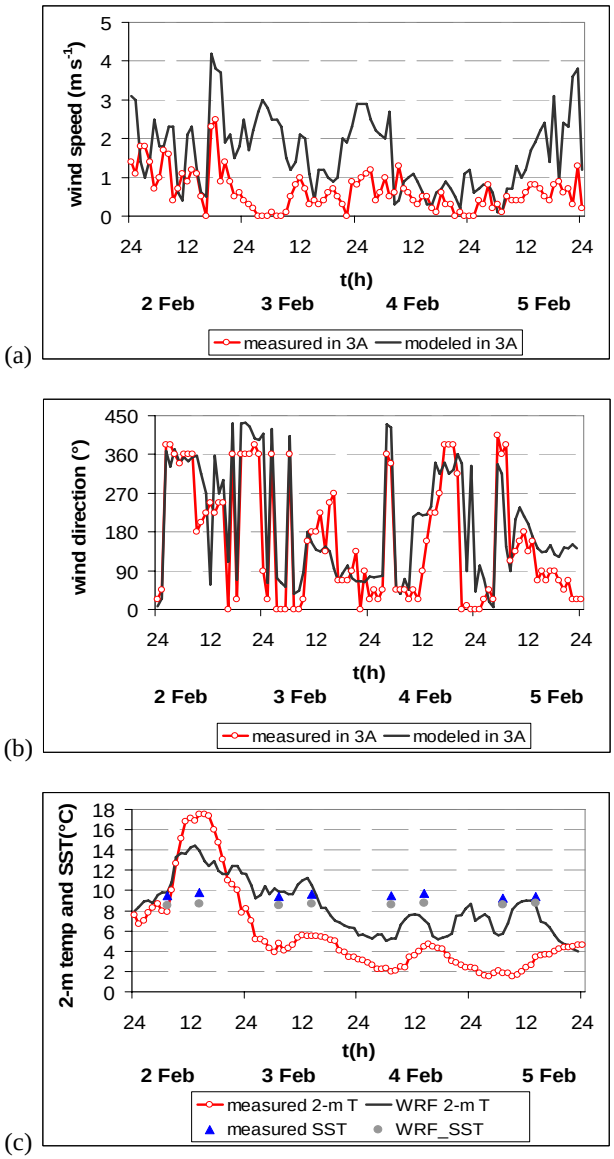

Fig. 6. The wind speed **(a)**, wind direction **(b)**, air temperature at 2 m height **(c)** from measurements (red line with circles) and WRF model simulations (black) in 3A (Rijeka) station from 2 February 2002, till 6 February 2002. At (c) panel blue triangles and grey circles correspond to the measured and WRF sea surface temperature (SST), respectively.

lands of Krk and Cres, as well as inside the Velebit channel (VC in Fig. 1), the northerly channelled flows were established.

During the evening hours of 2 February (20:00 UTC, Fig. 8), the airflow pattern at the western coast of Istria is similar to the daytime one (Fig. 7). The downstream flow still exists at the western slopes of the high mountains (Fig. 8). However, above the Rijeka Bay and the island of Krk, the wind regime started to change. As of 17:00 UTC

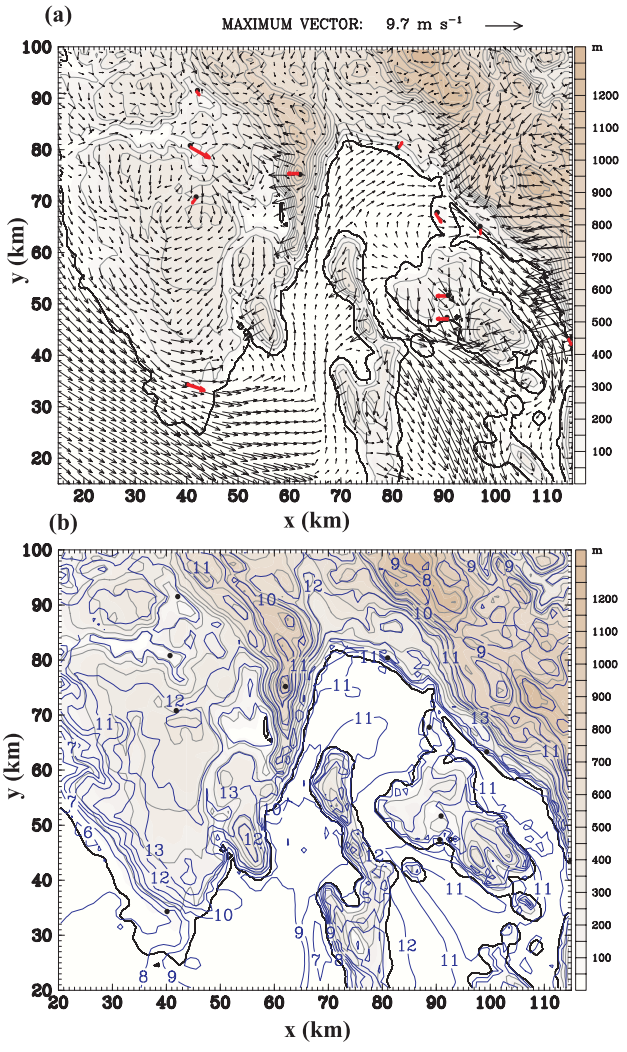

Fig. 7. **(a)** The measured (red arrows) 10-m wind ($m\,s^{-1}$) from main and ordinary meteorological stations in Table 1 and modelled WRF wind field (black arrows) as well as **(b)** WRF surface air temperature in °C on 2 February 2002 at 13:00 UTC. Note that the meteorological fields are shown in the enlarged finest WRF domain in order to show better the GRA area.

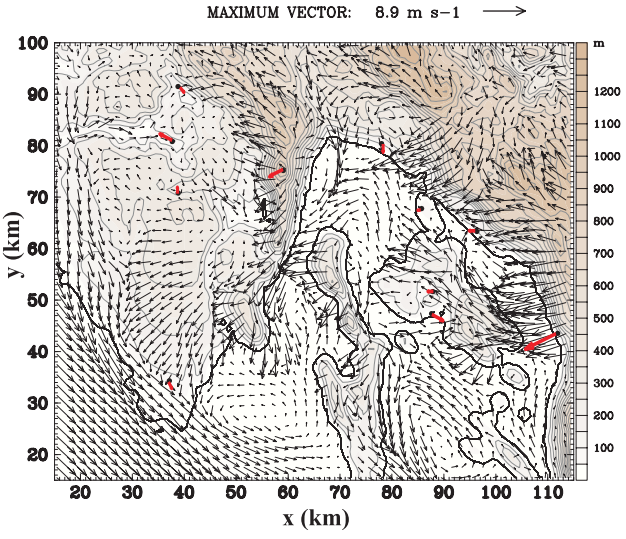

Fig. 8. The measured (red arrows) 10-m wind ($m\,s^{-1}$) from main and ordinary meteorological stations in Table 1 and modelled WRF wind field (black arrows) on 2 February 2002 at 20:00 UTC.

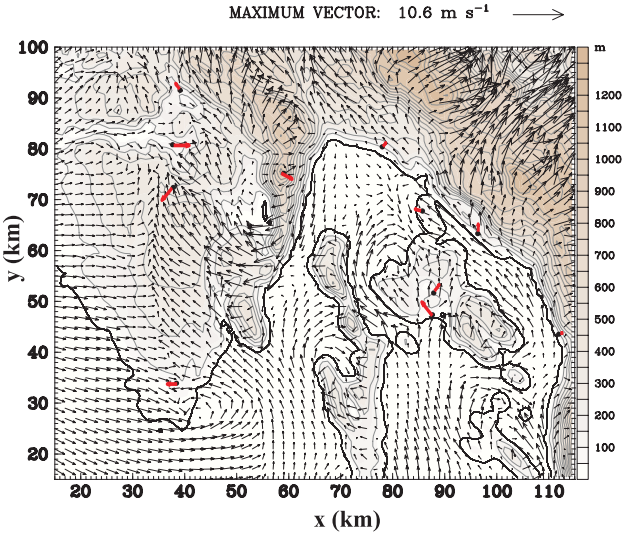

Fig. 9. Same as Fig. 7 except on 3 February 2002 at 13:00 UTC.

(not shown here) the anti-clockwise mesoscale eddy, associated with katabatic winds channelled within the pass between Risnjak and Velika Kapela, extends over the greater Rijeka area. A similar wind pattern, which is due to topography, has already been suggested by Prtenjak et al. (2006) for the night time stable conditions during summer. Above the island of Krk, especially over its eastern part (Fig. 8), south-easterly winds blow. Thus, they transport the air from the northern Krk, where the petrochemical plant and the oil terminal are located (point 2, Fig. 1c) towards the Rijeka town. Further, the established mesoscale vortex transports the air from the industrial zone of Rijeka (point 1, Fig. 1c) towards the town (Fig. 8). The transport of air above the areas with major pollution sources is accompanied by a gradual increase of atmospheric stability due to the nighttime cooling (not shown).

On 3 February, measurements show weak winds over Rijeka throughout the day. Over the western part of the Istria peninsula, easterly winds blow in the morning; south-easterly ones around noon, and eventually in the evening they vary randomly from northerly to easterly ones (not shown). In the central part of Istria wind directions are almost "frozen" in time, while magnitude slightly varies. Figure 9 depicts the observed and modelled winds for 3 February at 13:00 UTC. The modelled winds are up to about $4\,m\,s^{-1}$ over the entire coastal zone. Further, the cyclonic eddy is

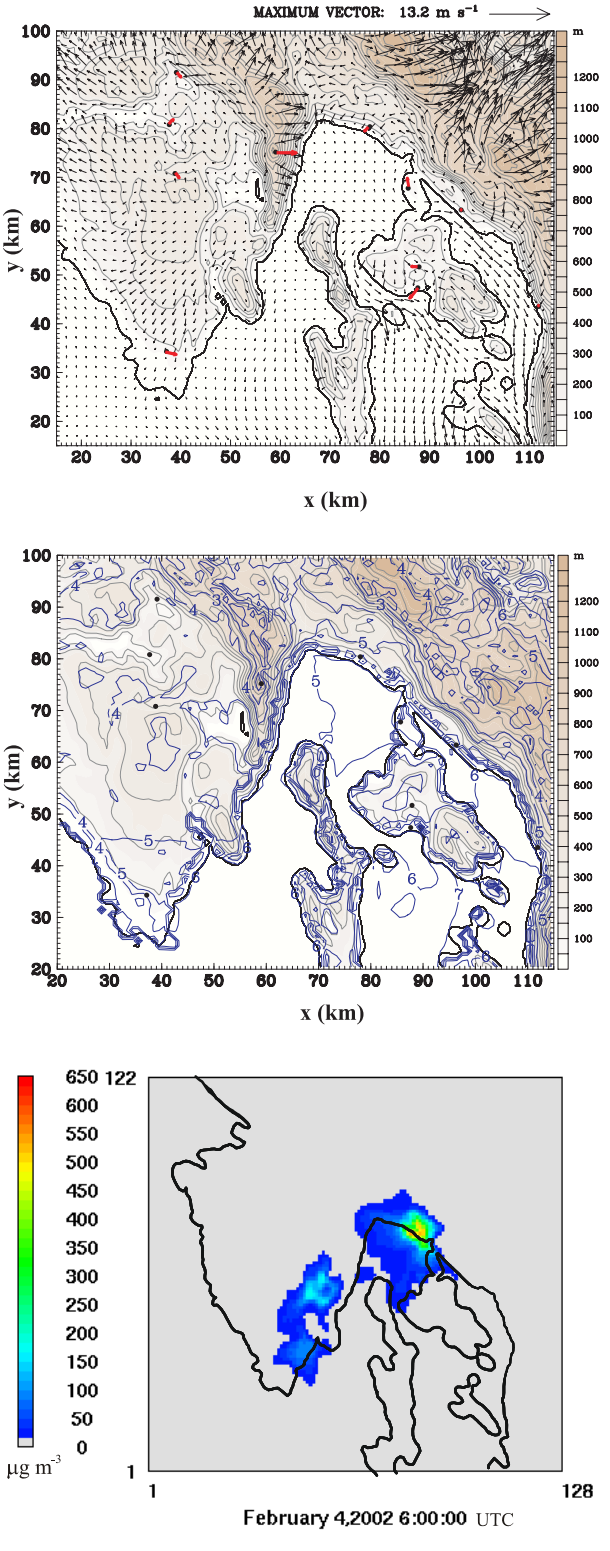

Fig. 10. **(a)** The measured (red arrows) 10-m wind ($m\,s^{-1}$) from main and ordinary meteorological stations in Table 1 and modelled WRF wind field (black arrows) as well as **(b)** WRF surface air temperature in °C on 4 February 2002 at 06:00 UTC. **(c)** Horizontal cross section at 55 m a.g.l. at 06:00 UTC for the SO_2 concentration in $g\,m^{-3}$ (colour scale) simulated by 1-km air quality model.

almost continuously present above the Rijeka Bay (Fig. 9). Bearing in mind the low wind speeds, the agreement between the measured and simulated wind vectors is satisfactory, with discrepancies at the southern tip of Istria being somewhat larger. According to the modelled wind fields, over the western coast of Istria, the westerly flow continues bringing the moist marine air over land. This further supports the persistence of fog, which according to measurements was reported for all coastal sites. Similarly, the previous evening, the modelled wind field exhibits a south-easterly flow which transports the air from local emission sources towards Rijeka town (Fig. 9). It is important to note that the airflow pattern over the greater Rijeka Bay area, in Fig. 9, is almost stationary throughout the 3 February. On the other hand, in the mountain pass between Ćićarija and Risnjak, the airflow conditions change and winds turn to south-easterly ones. Modelled temperatures are generally higher than measured ones (not shown). Further, the modelled temperature field pattern is similar to the pattern of the previous day, although the values are somewhat lower. In time, the atmosphere becomes more stable due to continuous nighttime radiative cooling of the land. The stable stratification suppresses the vertical mixing inside the boundary layer, which results in very weak nighttime winds especially above the Kvarner Bay. Over the major part of the Istrian peninsula, the modelled airflow is eastern, which agrees well with the measurements. The synoptic forcing is weak. Hence, both the complex topography and the stable stratification strongly influence the local winds.

During the night and morning hours of 4 February, stagnant surface wind conditions persisted almost everywhere in the coastal area. At 06:00 UTC (Fig. 10), over the major portion of Istria weak easterly winds are present and downslope flows are established over the eastern slopes of the Ćićarija, Učka, Velika Kapela and Velebit mountains. North of Rijeka, the drainage winds of cold surface air are blocked upon reaching a relatively warmer sea (Fig. 10). The existence of the weak south-easterly winds above Omišalj that veer toward easterly winds above Rijeka can still be noted until 12:00 UTC (not shown) in the about 400 m deep surface layer. These fairly weak winds likely support the air-mass stagnation and the pollutant accumulation in the lower atmospheric layer above Rijeka, thus resulting in the highest daily measured SO_2 concentration (Fig. 10c). Stagnant winds and overall weak synoptic forcing favour fog formation and short-lasting drizzle, which were reported for the coastal sites. Fog and drizzle are generally associated with strong static stability, which was found in this particular region (see Figs. 14 and 16). According to model results, as of 4 February at 13:00 UTC atmospheric conditions gradually changed and a north-westerly flow of moderate intensity started to establish in the GRA (Fig. 11). Therefore, there were no more conditions supporting the transport of air from the industrial areas towards the Rijeka town. Specifically, the wind became channelled by the island of Cres and Istria.

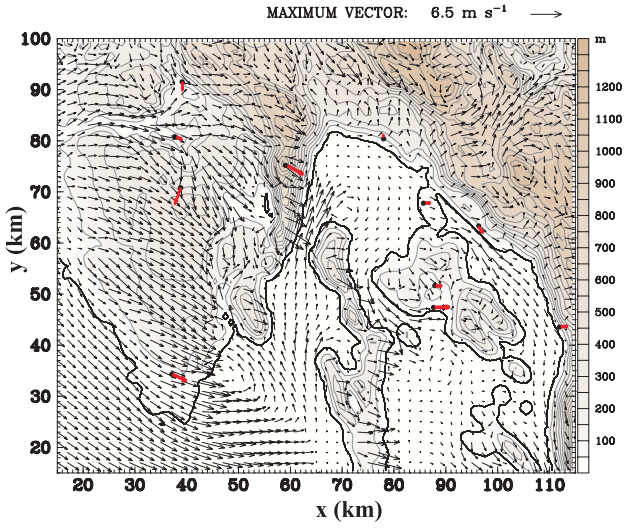

Fig. 11. Same as Fig. 7 except on 4 February 2002 at 13:00 UTC.

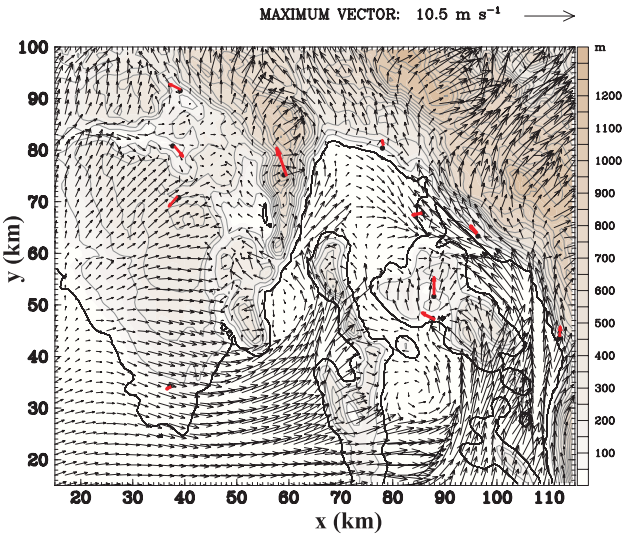

Fig. 12. Same as Fig. 7 except on 5 February 2002 at 13:00 UTC.

Thus, a very weak clockwise eddy forms, which transported air towards the island of Krk, and cancelled any earlier anticlockwise vortex inside the Rijeka Bay. The same is confirmed by measurements (Fig. 11). Generally, wind speeds remained lower than $5\,m\,s^{-1}$ until the 20:00 UTC. The airflow strengthened afterwards, especially over the southern tip of the Istria peninsula.

The afternoon wind distribution of the previous day mostly retains until 07:00 UTC of 5 February (not shown). Around noon, the CW eddy within the Rijeka Bay starts to diminish and south-easterly winds form through the Velebit channel. In the afternoon prevailing southerly winds dominate in the whole studied area (Fig. 12) changing the atmospheric conditions. In the GRA, winds fortify until the end of the day. This is in agreement with the decrease in SO_2 concentrations on 5 February (Fig. 3).

5.2.3 Vertical cross-sections

Modelled vertical cross-sections of potential temperature and wind vectors at 08:00 UTC and 17:00 UTC on 3 February are presented in Fig. 13. Here, the analysis is concentrated on the GRA regarding static stability and wind field. At 08:00 UTC (Fig. 13a) a different boundary layer development can be noted above the coast compared to adjacent foothills. The coastal shallow (≈200 m deep) stable layer is under the influence of the incoming south-easterly flow (Fig. 13b). A somewhat less stable layer is formed north-eastward (region above 27 km$<\times<$34 km in Fig. 13a) which is characterized by local mixing, with a subsidence above the sea and an upslope flow along the foothill above Rijeka. During the day, the difference between the ground-based layers above the Rijeka and adjacent foothills disappears and static stability increases (Figs. 13c, d). Under such circumstances, air ventilation is poor and winds are week. However, the southern airflow component persists further supporting the transport of air from industrial regions towards Rijeka. Further, it is interesting to notice the circulation cell, approximately 350 m deep, which is found between the mainland and the island of Cres above the lowermost approximately 100 m (bottom panel, right). This circulation cell in the vertical plain acts as a lid, which prevents the pollutants in the lowermost ground-based layer to dilute. During the night time, due to persistent subsidence and radiative cooling, the static stability increases (not shown), which further favours the pollutant accumulation in the lowermost atmospheric layers. Such pollution episodes, due to temperature inversions resulting in the stagnant air, have already been observed elsewhere (e.g. Fisher et al., 2005).

As stated above, during the first part of 4 February, the weak anticlockwise surface wind eddy still exists above the major portion of the Rijeka Bay. Thus, the transport of air from both the northern part of the island of Krk and the industrial zone southeast of town, continues, although south-easterly winds are rather weak. Simultaneously, apart from confirming the existence of south-easterly winds, the vertical fields (Fig. 14a and b, for 07:00 UTC) reveal further increase of the static stability over Rijeka, which is accompanied with the subsidence. Thus, the maximum daily mean SO_2 which is recorded on 4 February, can be attributed to the shallow and very stable ground-based layer with generally weak, predominantly south-eastern winds found in the first 200 m of the troposphere (Fig. 14c and d). In the afternoon hours (Fig. 14e, f), the wind direction changes, and subsidence over the Rijeka region, in the elevated layer extending from about 200 m to 1 km, increases. Consequently, the static stability within this layer also increases and further prevents pollutant dilution within the layer below (i.e. within the

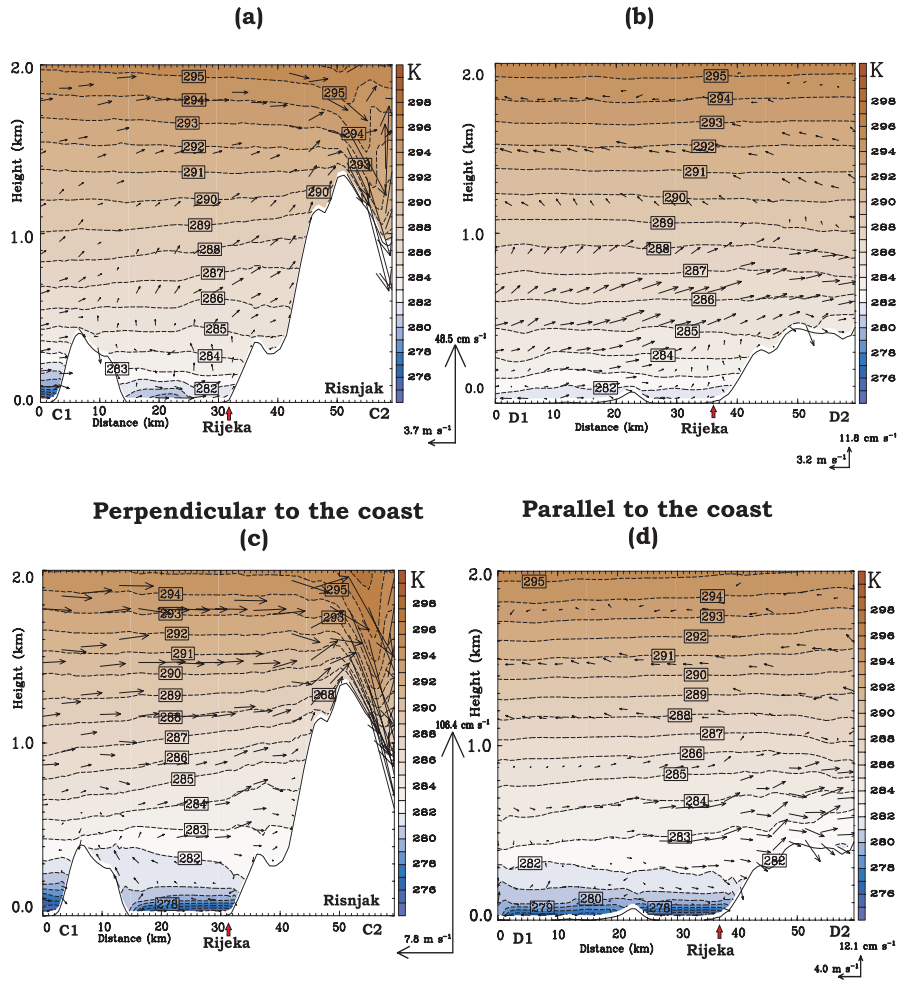

Fig. 13. Vertical cross-sections of the WRF modelled wind ($m\,s^{-1}$) and potential temperature (K) above Rijeka on 3 February 2002 at 08:00 UTC **(a, b)** and 17:00 UTC **(c, d)**. Left and right panels correspond to the cross-sections perpendicular (C1C2) and parallel (D1D2) to the coastline. Bases of the cross-sections are shown in Fig. 1b.

lowermost layer). In addition, winds in the lowermost layer remain weak. Accordingly, the SO_2 concentrations (Fig. 3) remain high until midday of 5 February. The vertical fields on 5 February show once more the daytime south-easterly winds above the major portion of the GRA (Fig. 15). The transport of air from both, the northern part of the island of Krk and the industrial zone southeast of the town is established again. However, the winds become stronger and static stability decreases over Rijeka (especially during the evening hours) which agrees with the decreasing in of the SO_2 concentrations (Fig. 3).

5.2.4 Potential temperature profiles and boundary layer heights

The evolution of vertical profiles of potential temperature from 2 to 5 February above Rijeka is shown in Fig. 16. The ground-based temperature inversion, which is present on 3 February at 08:00 UTC in the first 200 m, strengthens in time. Above the lowermost layer, the most stable one, another stable layer of somewhat weaker static stability exists. In time, its stability also increases up to the 4 February reaching the maximum stability. Conditions on 5 February are characterised by a decrease of SO_2 concentrations, lower static stability in the morning and relatively high mixing in the evening.

The daily course of the PBL height above Rijeka during the pollution episode is shown in Fig. 17. According to the model setup (MYJ scheme), the PBL is described by the one-dimensional prognostic turbulent kinetic energy scheme with local vertical mixing. Therefore, the PBL top depends on the TKE as well as the buoyancy and shear of the driving flow. In the stable range, the upper limit of the PBL is deduced from the requirement that the ratio of the variance of the vertical velocity deviation and the TKE cannot be smaller than that corresponding to the regime of vanishing

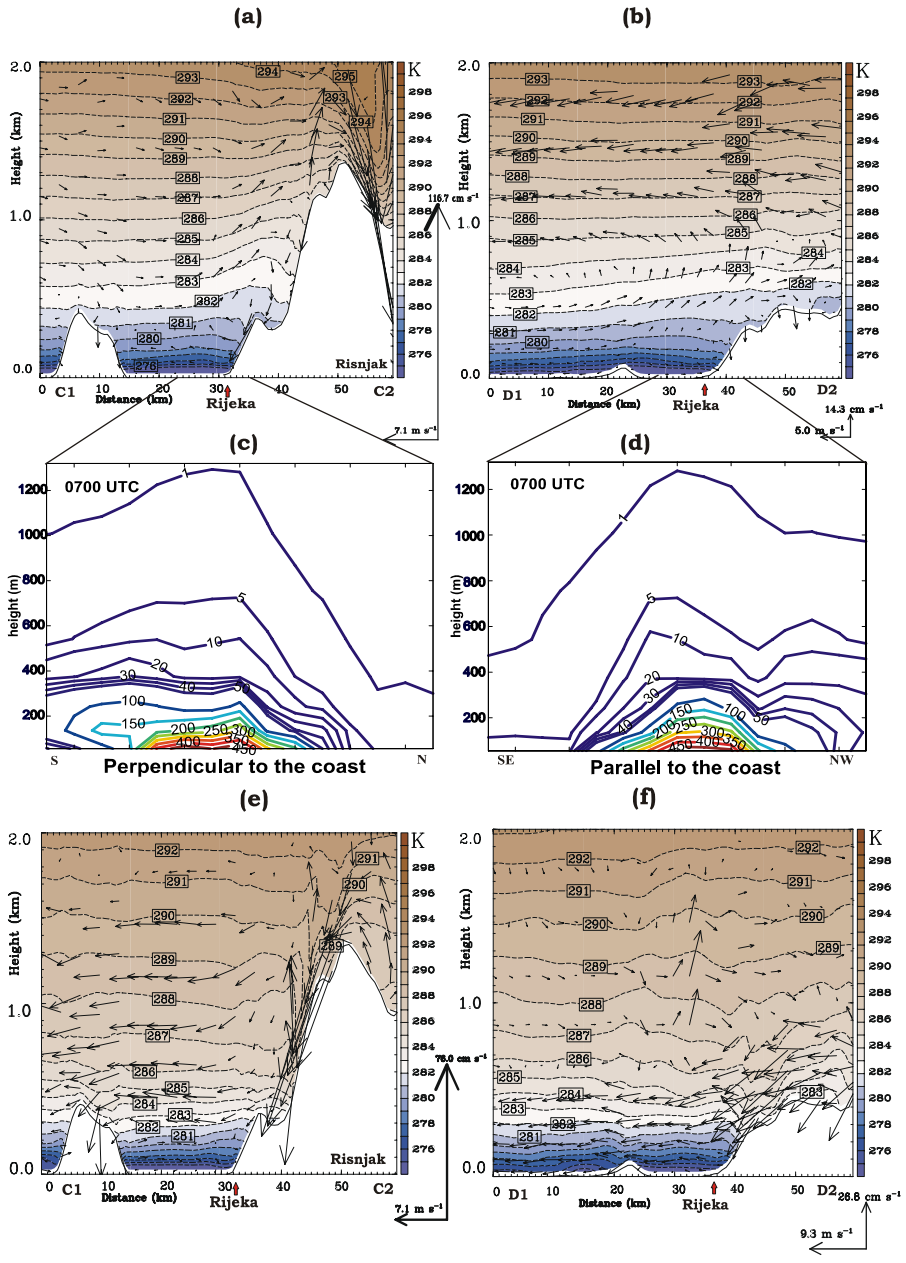

Fig. 14. Same as Fig. 13 except on 4 February 2002 at 07:00 UTC **(a, b)** and 18:00 UTC **(e, f)**. A close-up of the vertical distribution of the SO_2 concentrations ($\mu g\,m^{-3}$) simulated by the chemical model at 1-km resolution at 07:00 UTC along **(c)** C1C2 and **(d)** D1D2 cross-sections around Rijeka area.

turbulence (http://www.wrf-model.org/index.php). According to the modelled PBL height of Rijeka, the daily maximum on 2 February were around 900 m. Higher air temperatures above Rijeka are connected to the higher boundary layer. According to Jeričević et al. (2004), this can result in the pollutant entrainment into the boundary layer from a residual layer from the previous day. However, tracking of modelled pollutant concentrations at elevated levels, we did not find the confirmation of this hypothesis. The maximum SO_2 concentration was in the lowermost layer during the episode (as seen from the Fig. 14c–d). The next day, the maximum PBL height was up to about 400 m. On 4 February, which is characterized by both, the maximum daily SO_2 concentration and the maximum static stability, the PBL height was up to about 140 m. For the same period, Jeričević et al. (2004) obtained more periodically and much higher mixing heights. The conclusion was that the ALADIN model unrealistically overpredicted 2-m air temperature for days with

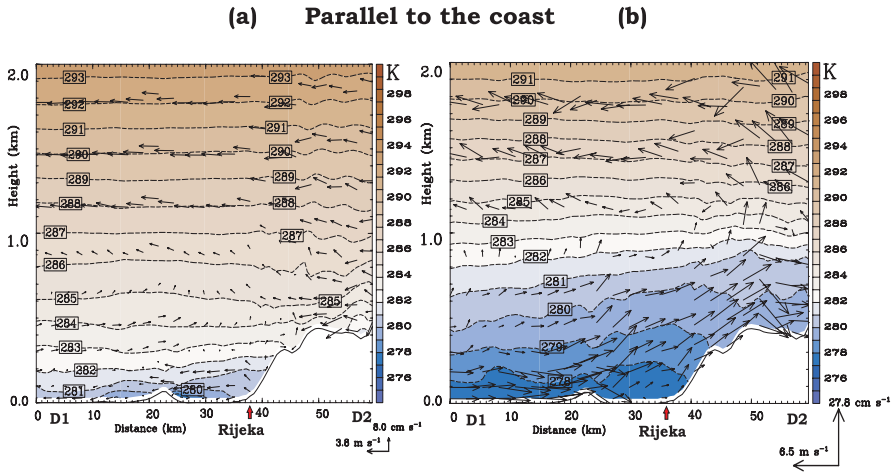

Fig. 15. Vertical cross-sections of the WRF modelled wind ($m\,s^{-1}$) and potential temperature (K) above Rijeka on 5 February 2002 at 07:00 UTC **(a)** and 18:00 UTC **(b)** along parallel cross-section (A1) to the coastline. Base of the D1D2 cross-section is shown in Fig. 1b.

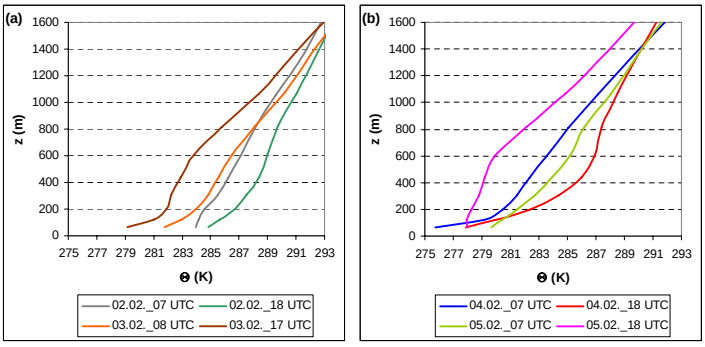

Fig. 16. Modelled WRF vertical profiles of potential temperature (K) from 2 to 5 February 2002 above Rijeka. Times correspond to the times of cross-sections shown in Figs. 13–15.

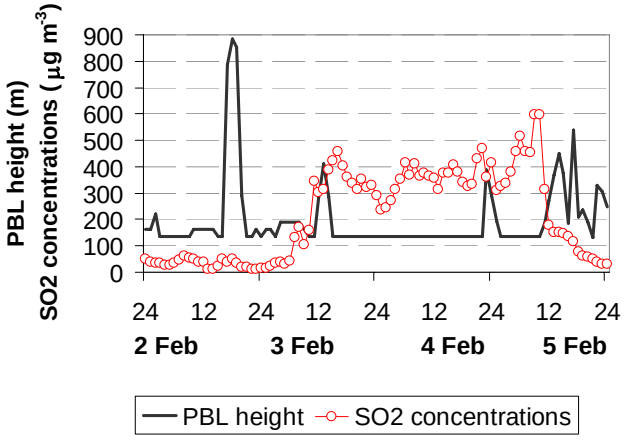

Fig. 17. The daily course of the modelled WRF planetary boundary layer height (m) (black) obtained for Rijeka as well as measured SO_2 concentrations for Rijeka (red circles) (site 3B in Table 1 and Fig. 1b) from 2 to 6 February 2002 (source for SO_2 measurements: Teaching Institute for Public Health, Rijeka).

fog, giving mixing height maxima around 400 m. The hourly modelled SO_2 concentrations explicitly follow PBL height and associated meteorological conditions (especially compare CAMx results in Fig. 3 and Fig. 17). The increase in measured concentrations goes along with the modelled PBL height decrease (Fig. 17). Likewise, on 5 February, the increase of the PBL height and the decrease of the static stability (Fig. 16) results in the hourly SO_2 concentrations decrease after 10:00 UTC (Fig. 17).

6 Conclusions

We examined the relationships between meteorological fields and high SO_2 concentrations recorded on 3–5 February 2002 in the coastal town of Rijeka. Although the hourly concentrations gradually grew toward the highest value on 5 February, the maximum daily mean SO_2 concentration occurred on 4 February causing very dangerous health conditions for the inhabitants of Rijeka. The episode took place during high pressure conditions. Then, the maximum air temperatures were

mostly lower than the sea surface temperatures, and the diurnal air temperature amplitude was low (around 3°C). Under such circumstances fog developed along the coast and wind speeds were very low.

Results of three air quality models at horizontal resolutions of 50, 10 and 1 km, for the EMEP, EMEP4HR and CAMx, respectively, suggested the major role of the local pollution sources in the establishment of pollution episode, while contribution from distant sources in Bulgaria, Bosnia and Italy to the overall recorded SO_2 concentration was relatively small (up to about 10%).

The episode was caused by specific, local-scale meteorological conditions, which could not be captured by 50-km and 10-km resolution meteorological drivers of EMEP and EMEP4HR, respectively. However, both fine-scale (at resolution of 1 km) meteorological (WRF) and air quality model (CAMx) results demonstrated a successful multi-day simulation in the GRA and reasonable agreement with the available observations.

The WRF model results suggest several factors responsible for the occurrence of the severe pollution episode. These are as follows.

- Transport of air from nearby pollution sources within the GRA towards Rijeka by south-easterly winds. These surface winds are often connected to the anti-clockwise eddy inside the Rijeka Bay, which maintains the transport of polluted air from the Rijeka industrial zone (oil refinery and thermo-power plant) and the island of Krk especially over its northern part, where the, petrochemical plant and the oil terminal are located.

- The abovementioned transport of air from the areas with major pollution sources was accompanied by a gradual increase of atmospheric stability during the episode. The maximum static stability occurred on 4 February limiting the dispersion of pollutants in the very low (within 140 m) mixing layer. The mixing layers were associated by the formation of a strong ground-based radiation inversion in the GRA.

- The surface wind field shows the stagnation region of airflow upstream of Rijeka which is favourable of pollutant accumulation (especially during 4 February, see Fig. 14e).

- The air subsidence in the lowermost layer south of Rijeka, further facilitates pollutant accumulation. The subsidence is a result of the circulation cell, approximately 500 m deep, which is found between the mainland and the island of Cres above the lowermost approximately 100 m (on 3 February). This circulation cell in the vertical plain acts as a lid, which prevents the pollutants in the ground-based layer to dilute. During the next day, the drainage flow occurred above the circulation cell that existed in the first 200 m where the wind profile exhibited calm or lower wind less than $1\,m\,s^{-1}$. The drainage flow was related to the increase of wind speed enhancing static stability above Rijeka.

Weak winds and calms are frequent in Rijeka (e.g. Prtenjak and Grisogono, 2007), and they are not always accompanied by elevated pollutant concentrations. However, this episode was characterized by extremely low winds (wind speeds were mostly below $1\,m\,s^{-1}$ with the maximum of $1.3\,m\,s^{-1}$) accompanied with high static stability and prominent subsidence. Thus, simultaneous occurrence of all these phenomena, together with the airflow from industrial zones toward Rijeka town were responsible for the episode severity. Finally, it can be summarized that that local meteorological conditions were extremely favourable for the formation of this severe pollution episode.

Acknowledgements. Three anonymous referees are acknowledged for their useful suggestions. We are grateful to Teaching Institute for Public Health, Rijeka for SO_2 data and Ana Alebić-Juretić (from the same Institute) for available comments. Also, we are indebted to the Meteorological and Hydrological Service of the Republic of Croatia and the Meteorological Department of the Croatian Air Traffic Control at Zagreb Airport for providing the meteorological data. This work has been supported by the Ministry of Science, Educational and Sport (grants No. 119-1193086-1323, No. 119-1193086-1311 and No. 004-1193086-3036) and EMEP4HR project number 175183/S30 provided by the Research Council of Norway.

Edited by: D. Simpson

References

Baklanov, A. and Grisogono, B.: Amospheric boundary layers: nature, theory and applications to environmental modeling and security, Springer, 241 pp., 2007.

Bott, A.: A positive definite advection scheme obtained by nonlinear renoramlization of the advection fluxes, Mon. Weather Rev., 117, 1006–1015, 1989a.

Bott, A.: A positive definite advection scheme obtained by nonlinear renormalization of the advective fluxes – reply, Mon. Weather Rev., 117, 2633–2636, 1989b.

Brulfert, G., Chemel, C., Chaxel, E., and Chollet, J. P.: Modelling photochemistry in alpine valleys, Atmos. Chem. Phys., 5, 2341–2355, 2005, http://www.atmos-chem-phys.net/5/2341/2005/.

de Foy, B., Lei, W., Zavala, M., Volkamer, R., Samuelsson, J., Mellqvist, J., Galle, B., Martínez, A.-P., Grutter, M., Retama, A., and Molina, L. T.: Modelling constraints on the emission inventory and on vertical dispersion for CO and SO_2 in the Mexico City Metropolitan Area using Solar FTIR and zenith sky UV spectroscopy, Atmos. Chem. Phys., 7, 781–801, 2007, http://www.atmos-chem-phys.net/7/781/2007/.

De Leeuw, F. A. A. M. and Leyssius, H. J. V.: Long-range transport modelling of air pollution episodes, Environ. Health Perspect., 79, 53–59, 1989.

Drobinski, P., Said, F., Arteta, J., Augustin, P., Bastin, S., Brut, A., Caccia, J. L., Campistron, B., Cautenet, S., Colette, A., Coll, I., Corsmeier, U., Cros, B., Dabas, A., Delbarre, H., Dufour, A., Durand, P., Guenard, V., Hasel, M., Kalthoff, N., Kottmeier, C., Lasry, F., Lemonsu, A., Lohou, F., Masson, V., Menut, L., Moppert, C., Peuch, V. H., Puygrenier, V., Reitebuch, O., and Vautard, R.: Regional transport and dilution during high-pollution episodes in southern France: Summary of findings from the Field Experiment to Constraint Models of Atmospheric Pollution and Emissions Transport (ESCOMPTE), J. Geophys. Res.-Atmos. 112, D13105, doi:10.1029/2006JD007494, 2007.

ENVIRON: User's guide: CAMx comprehensive Air Quality model with Exstensions, Version 4.50. ENVIRON International Corporation, Novato, CA, 2008.

Evtyugina, M. G., Nunes, T., Pio, C., and Costa, C. S.: Photochemical pollution under sea breeze conditions, during summer, at the Portuguese West Coast, Atmos. Environ., 40, 6277–6293, 2006.

Fagerli, H., Simpson, D., and Tsyro, S. Unified EMEP model: Updates Transboundary acidification, eutrophication and ground level ozone in Europe. EMEP Status Report 1/2004, The Norwegian Meteorological Institute, Oslo, Norway, 11–18, 2004.

Fisher, B., Joffre, S., Kukkonen, J., Piringer, M., Rotach, M. W., and Schatzmann, M. (Eds.): Meteorology applied to Urban Air Pollution Problems, Final Report COST Action 715, Demetra Ltd. Publishers, Bulgaria, 2005.

Geleyn, J. F., Banciu, D., Bubnova, R., Ihasz, I., Ivanovici, V., LeMoigne P., and Radnoti, G.: The International Project ALADIN: Summary of Events October 1992–October 1993, LAM Newsletter 23, 1992.

Gery, M. W., Whitten, G. Z., Killus, J. P., and Dodge, M. C.: A photochemical kinetics mechanism for urban and regional scale computer modelling, J. Geophys. Res., 94, 925–956, 1989.

Grisogono, B., Kraljević, L., and Jeričević, A.: The low-level katabatic jet height versus Monin-Obukhov height, Q. J. Roy. Meteorol. Soc., 133, 2133–2136, 2007.

Jeričević, A., Špoler Čanić K., and Vidič, S.: Prediction of stability and mixing height in the complex orography, Cro. Meteorol. J., 39, 3–14, 2004.

Jeričević, A., Kraljević, L., Vidič, S., and Tarrason, L.: Project description: High resolution environmental modelling and evaluation programme for Croatia (EMEP4HR), Geofizika, 24, 137–143, online available at: http://geofizika-journal.gfz.hr/abs24_2.htm#25, 2007.

Jimenez-Guerrero, P., Jorba, O., Baidasanoa, J. M., and Gasso, S.: The use of a modelling system as a tool for air quality management: Annual high-resolution simulations and evaluation, Science Total Environ., 390, 323–340, 2008.

Kain, J. S., Weiss, S. J., Levit, J. J., Baldwin, M. E., and Bright, D. R.: Examination of convection-allowing configurations of the WRF model for the prediction of severe convective weather: The SPC/NSSL Spring Program 2004, Weather Forecast., 21, 167–181, 2006.

Klaić, Z.: A Lagrangian one-layer model of long-range transport of SO_2, Atmos. Envrion., 24A, 1861–1867, 1990.

Klaić, Z.: A Lagrangian model of long-range transport of sulphur with the diurnal variations of some model parameters, J. Appl. Meteorol., 35, 574–585, 1996.

Klaić, Z. B.: Assesment of wintertime atmospheric input of European sulfur to the eastern Adriatic, Nuovo Cimento, 26C, 1–6, 2003.

Klaić, Z. B and Beširević, S.: Modelled sulphur depositions over Croatia, Meteorol. Atmos. Phys., 65, 133–138, 1998.

Klaić, Z. B., Belušić, D., Grubišić, V., Gabela, L., and Ćoso, L.: Mesoscale airflow structure over the northern Croatian coast during MAP IOP 15 – a major bora event, Geofizika, 20, 23–61, 2003.

Klaić, Z. B., Pasarić, Z., and Tudor, M.: On the interplay between sea-land breezes and Etesian winds over the Adriatic, J. Marine Syst., in press, doi:10.1016/j.jmarsys.2009.01.016, 2009.

Levy, I., Dayan, U., and Mahrer, Y.: A five-year study of coastal recirculation and its effect on air pollutants over the East Mediterranean region, J. Geophys. Res.-Atmos, 113, D16121, doi:10.1029/2007JD009529, 2008.

Mahrt, L. and Vickers, D.: Extremely weak mixing in stable conditions, Bound.-Lay. Meteorol., 119, 19–39, 2006.

Mahrt, L.: The influence of nonstationarity on the turbulent flux-gradient relationship for stable stratification, Bound.-Lay. Meteorol., 125, 245–264, 2007.

Michalakes, J., Dudhia, J., Gill, D., Henderson, T., Klemp, J., Skamarock, W., and Wang, W.: The Weather Research and Forecasting Model: software architecture and performance, in: 11th ECMWF Workshop on the use of High Performance Computing in Meteorology, edited by: Mozdzynski, G., Reading, UK, 2004.

Natale, P., Anfossi, D., and Cassardo, C.: Analysis of an anomalous case of high air pollution concentration in Turin after a foehn event, Int. J. Environ. Pollut., 11, 147–164, 1999.

Nitis, T., Kitsiou, D., Klaić, Z .B., Prtenjak, M. T., and Moussiopoulos, N.: The effects of basic flow and topography on the development of the sea breeze over a complex coastal environment, Q. J. Roy. Meteorol. Soc., 131, 305–328, 2005.

O'Brien, J. J.: A Note on the Vertical Structure of the Eddy Exchange Coefficient in the Planetary Boundary Layer, J. Atmos. Sci., 27, 1213–1215, 1970.

Pohjola, M. A., Rantamaki, M., Kukkonen, J., Karppinen, A., and Berge, E.: Meteorological evaluation of a severe air pollution episode in Helsinki on 27–29 December 1995, Boreal Env. Res., 9, 75–87, 2004.

Prtenjak, M. T., Grisogono, B., and Nitis, T.: Shallow mesoscale flows at the north-eastern Adriatic coast, Q. J. Roy. Meteorol. Soc., 132, 2191–2215, 2006.

Prtenjak, M. T. and Grisogono, B.: Sea/land breezes climatological characteristics along the northeastern Adriatic coast, Theor. Appl. Climatol., 90, 201–215, doi:10.1007/s00704-006-0286-9, 2007.

Prtenjak, M. T., Pasarić, Z., Orlić, M., and Grisogono, B.: Rotation of sea/land breezes along the northeastern Adriatic coast, Ann. Geophys., 26, 1711–1724, 2008, http://www.ann-geophys.net/26/1711/2008/.

Robinsohn, J., Mahrer, Y., and Wakshal, E.: The effects of mesoscale circulation on the dispersion of pollutants (SO_2) in the eastern Mediterranean, southern coastal-plain of Israel, Atmos. Environ., 26, 271–277, 1992.

Skamarock, W. C., Klemp, J. B., Dudhia, J., Gill, D. O., Barker, D. M., Wang, W., and Powers, J. G.: A description of the Advanced Research WRF Version 2, NCAR/TN-468+STR, NCAR TECHNICAL NOTE, 88 pp., online available at: http://www.mmm.ucar.edu/wrf/users/docs/arw_v2.pdf, January 2007.

Skamarock, W. C. and Klemp, J. B.: A time-split nonhydrostatic

atmospheric model for weather research and forecasting applications, J. Comput. Phys, 227, 3465–3485, 2008.

Skouloudis, A. N., Kassomenos, P., and Nitis, T.: Science and policy challenges of atmospheric modelling in consideration of health effects, Int. J. Environ. Pollut., accepted, 2009.

Soler, M. R., Hinojosa, J., Bravo, M., Pino, D., and de Arellano, J. V. G.: Analyzing the basic features of different complex terrain flows by means of a Doppler Sodar and a numerical model: Some implications for air pollution problems, Meteorol. Atmos. Phys., 85, 141–154, 2004.

Steenkist, R.: Episodes of high SO_2 concentration in The Netherlands, Atmos. Environ., 22, 1475–1480, 1988.

Stull, R. B.: An introduction to boundary layer meteorology, Kluwer, Dordrecht, 1988.

Tayanc, M. and Bercin, A.: SO_2 modeling in Izmit Gulf, Turkey during the winter of 1997: 3 cases, Environ. Model. Assess., 12, 119–129, 2007.

Trenberth, K. E., Davis, C. A., and Fasullo, J.: Water and energy budgets of hurricanes: Case studies of Ivan and Katrina, J. Geophys. Res.-Atmos., 112, D23106, doi:10.1029/2006JD008303, 2007.

Vieno, M., Dore, A. J., Wind, P., Di Marco, C., Nemitz, E., Phillips, G., Tarrason, L., and Sutton, M. A.: Application of the EMEP Unified Model to the UK with a horizontal resolution of $5\times5\,km^2$, in: Atmospheric Ammonia: Detecting emission changes and environmental impacts, edited by: Sutton, M. A., Baker, S., and Reis, S., Springer, 464 pp., 2009.

Vieno, M., Dore, A. J., Stevenson, D. S., Doherty, R., Heal, M., Reis, S., Hallsworth, S., Tarrasón, L., Wind, P., and Sutton, M. A.: 'MODELLING SURFACE OZONE DURING THE 2003 HEAT WAVE IN THE UK, 'Croatian Meteorological Journal 43, The 12th International Conference on Harmonizaton within Atmospheric Dispersion Modelling for Regulatory Purposes, HARMO 12, Djuričić, V., Zagreb, Croatian Meteorological Society, 83–87, 2008.

Willmott, C. J.: Some comments on the evaluation of model performance, B. Am. Meteorol. Soc., 63, 1309–1313, 1982.

Wyngaard, J. C.: Toward numerical modeling in the "Terra Incognita", J. Atmos. Sci., 61, 1816–1826, 2004.